MOLECULAR MECHANICS OF CYTOSKELETAL COMPONENTS

M. Atakhorrami
Vrije Universiteit Amsterdam, Dept. Phys.
Amsterdam, The Netherlands

K.M. Addas
Rowland Institute at Harvard
Cambridge, MA, USA

M. Buchanan, G.H. Koenderink, F.C. MacKintosh
Vrije Universiteit Amsterdam, Dept. Phys.
Amsterdam, The Netherlands

J.X. Tang
Brown University, Dept. Phys.
Providence, RI, USA

Christoph F. Schmidt
Vrije Universiteit Amsterdam, Dept. Phys.,
Amsterdam, The Netherlands
cfs@nat.vu.nl

Abstract   Semiflexible polymers are of great biological importance in determining the mechanical properties of cells. We have used optical tweezers to trap pairs of micron-sized silica spheres in solutions of semiflexible polymers, and laser interferometry to detect their thermal motions with high bandwidth. Frequency-dependent complex shear moduli were extracted from the auto- and cross-correlated bead motions, with the response functions being derived from position-fluctuation data using dispersion relations from linear response theory.

Keywords: Cytoskeleton; semiflexible polymers; microrheology; optical tweezers; laser interferometry

1.   Introduction

One of the characteristic lengths that describes a polymer in a solution is the persistence length L_p, which is the length traversed along the filament contour before the tangent vector thermally randomizes its orientation. L_p is proportional to the bending stiffness of the polymer. Flexible polymers are characterized by $L_p << L$, rigid rod polymers by $L_p >> L$. Semiflexible polymers are in the intermediate regime, characterized by $L_p \approx L >> d$, with filament diameter d. The dynamics of polymer solutions and networks greatly depends on the degree of flexibility of the individual polymers. Recent theoretical treatments have addressed semiflexible polymer networks [1-4]. Such polymers are found particularly in biology where they form networks that determine the mechanical properties of cells.

We report here on rheology experiments on such polymer systems, and in particular on a new microrheology method. There are clear advantages to the miniaturization of a rheology experiment: only small amounts of material are necessary, spatial inhomogeneities can be studied, and the bandwidth of the measurement can be high. We have developed a microrheology technique using laser interferometric tracking of the Brownian motion of micron-sized beads embedded in viscoelastic materials [5]. The simplest implementation of the technique consists of tracking one probe particle at a time (1-bead microrheology) [5]. A further development, avoiding local artefacts due to the insertion of the probe particles into the system, consists of measuring the correlated fluctuations of pairs of probe particles (2-bead microrheology). We have studied the dynamics of several systems and have compared 1-bead and 2-bead results for wormlike micelle, semiflexible fd virus and actin solutions. Particularly in the actin systems, which is a first approximation to the cytoskeleton of cells, we explore the rich multitude of length and time scales in the dynamic behavior of these networks, which are not accessible to conventional macrorheology.

2.   Principle of the Technique

The microrheology (MR) technique used here is a passive one in which the thermal fluctuations of pairs of micron-sized beads are observed. Complex auto- and cross-correlation response functions of the beads are calculated using the fluctuation-dissipation theorem [5,6]. The complex response function $\alpha_{ij}^{(n,m)}(f)$ relates the Fourier transform $r_i^{(n)}(f)$ of the displacement of the nth bead $r_i^{(n)}(t)$ to the Fourier transform $F_j^{(m)}(f)$ of the force $F_j^{(m)}(t)$ acting on the mth bead (i and j are either 1 or 2 for

the parallel and perpendicular directions with respect to the line joining the bead centers, respectively),

$$r_i^{(n)}(f) = \alpha_{ij}^{(n,m)}(\vec{r}, f)F_j^{(m)}(f). \tag{1}$$

The measured response function must first be corrected for the trapping effect of the optical tweezers [7]. The fluctuation-dissipation theorem [5] provides the link between the single-sided power spectral density (PSD) [8]

$$S_{ij}^{(n,m)}(f) = \lim_{t' \to \infty}(2/t)r_{t'i}^{(n)}(f)r_{t'j}^{(m)*}(f) \tag{2}$$

and the imaginary part of the response function, where $r_{t'i}^{(n)}(f)$ is the Fourier transform of the position $r_i^{(n)}(t)$, defined over a finite time t'. A Kramers-Kronig integral can then be used to calculate the real part of the response function, provided that the imaginary part is known over a large enough frequency range. The connection between the auto-correlation response $\alpha_{ii}^{(n,m)}(f)$ of a bead and the corresponding complex shear modulus

$$G_{ii}^{(n,m)}(f) = G_{ii}'^{(n,m)}(f) + iG_{ii}''^{(n,m)}(f) \tag{3}$$

of the viscoelastic medium surrounding the bead is assumed to be provided by the generalized Stokes-Einstein relation (GSER) [5],

$$G_{ii}^{(n,m)}(f) = \frac{1}{[6\pi a\alpha_{ii}^{(n,m)}(f)]}, \tag{4}$$

where G' and G'' are the elastic and loss modulus respectively, and a is the radius of the bead. The cross-correlation shear modulus of the solution is derived from the parallel $a_{\parallel} \equiv \alpha_{11}^{(1,2)}$ response by [9]

$$G_{\text{cross}}(f) = \frac{1}{[4\pi r\alpha_{\parallel}(f)]}, \tag{5}$$

where r is the distance between the centers of the beads.

3.   Experimental Setup

Two focused laser beams were used to form optical tweezers and trap pairs of probe particles imbedded in solutions of semiflexible polymers. Position fluctuation data was recorded with a 200 kHz sampling rate, using laser interferometry and quadrant photodiode detection as described in detail elsewhere [5,6,10]. A near-infrared (1064 nm) laser was used for one trap and a 830 nm laser for the second trap. The beams
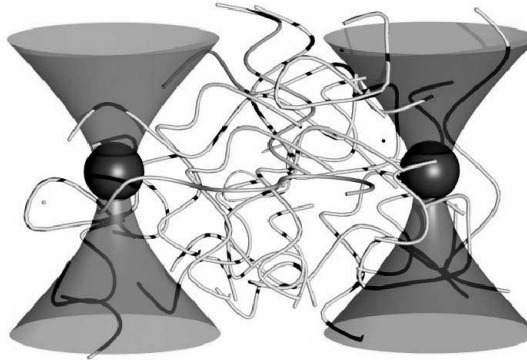
Figure 1.   Schematic illustration of the 2-bead microrheology experiment. Two spheres of radius a, are held in two optical tweezers, created by focusing lasers of different wave lengths $\lambda = 830\,\text{nm}$ and $\lambda = 1064\,\text{nm}$ at a separation distance r. The displacements of both particles are detected separately in x and y direction with interferometry.

are brought to a focus in the sample chamber by a high numerical aperture objective. The laser light emerging from the condenser lens, after passing through the sample, is projected onto two quadrant photodiodes in such a way that the back-focal plane of the condenser is imaged [10]. The signals from the four quadrants of each photodiode are combined to obtain the X- and Y-voltages corresponding to the displacements of each bead in these directions in the plane normal to the propagation direction of the laser. The output voltages are, after analog amplification and pre-processing, recorded using an A/D interface and digital data acquisition.

4.   Results

Worm-like Micelle Solutions

Figure 2 presents the loss and the viscous shear modulus of a worm-like micelle solutions for 1wt % concentration. The worm-like micelle solutions were made of binary mixtures of cetylpyridium chloride (CPyCL) and sodium salicylate (NaSal) dissolved in brine (0.5 M NaCl). A characteristic feature of worm-like micelle solutions is that they relax low-frequency applied stress with a single dominant relaxation time, reflecting breakage and reptation of the filaments [11]. The system we used
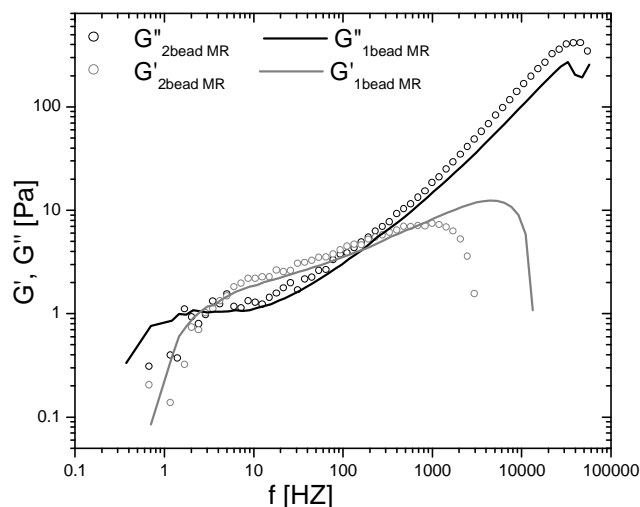
Figure 2.   Elastic modulus and loss modulus for a 1wt% worm-like micelle solution. Figure shows the comparison of 1-bead and 2-bead microrheology. The diameter of the beads was $D = 2.1\,\mu$m.

produces micelles with typical diameters of 2-3 nm, a persistence length L_p 10 nm, and an average length between 100 nm and 1 μm. We have performed 1-bead MR and 2-bead MR for different concentrations of micelles. Bead diameters were 1.16 μm and 2.1 μm.

For this system 1-bead and 2-bead MR results show excellent agreement (Fig. 2). More experimental noise is usually found in 2-bead results since the cross-correlation signal between the displacement of two beads is always weaker than the auto-correlation signal of one bead. The abrupt decrease in both G' and G'' at high frequncies is artefactual and due to anti-alias filtering at the Nyquist frequency and to the finite frequency cut-off effects on the result of the Kramers-Kronig integral. The effect on G' is stronger than on G'', reflected in about a decade less usable data for G' [5].

It is expected that 1-bead measurements could be sensitive to the local medium properties in the direct vicinity of the probe bead, which could be different from bulk properties due to surface chemistry or steric (entropic) effects. The unmodified bulk viscoelastic properties of the solutions should, on the other hand, be reported by the 2-bead results [9]. Even in the absence of specific chemical or electrostatic interactions, steric depletion of polymer in the vicinity of the probe particles is expected to cause differences in the 1- and 2-bead results, provided that probe size and network length scales are comparable. In the case of

6   *ICTAM04*

the worm-like micelle solutions we studied here, network length scales
are at least a decade smaller than bead radius and we therefore did not
expect differences due to surface artefacts. The data nicely confirms
this expectation and confirms the validity of both methods. It should
be noted that independently measured parameters enter the data eva-
luation for the two cases, bead diameter for 1-bead results and bead
distance (only) for 2-bead results. These results further establish mi-
crorheology, both 1-bead and 2-bead methods, as a highly sensitive and
high-bandwidth technique to measure shear elastic moduli of viscoelastic
materials. Good agreement between more conventional macrorheology
and microrheology on similar samples is reported elsewhere [12].

Fd Virus Solutions

Fd virus is a filamentous DNA bacteriophage [6], which is here used
as a monodisperse model system for semiflexible polymers. Filaments
have a diameter of 7 nm, persistence length $L_p = 2.2\,\mu$m and contour
length $L = 0.9\,\mu$m. Fd solutions were probed with a bead diameter of
$D = 1.16\,\mu$m. Fig. 3(a) shows the concentration dependence of the 1-
bead (circles) and 2-bead (triangles) elastic moduli. The loss modulus is
shown in Fig. 3(b). Data are displayed for 2, 5, 10, and 14 mg/ml fd con-
centrations. The high-frequency slope of the loss modulus is consistent
with single filament dynamics predictions [1,4]. At such high frequen-
cies, the entanglement of the polymer in its network does not contribute
to the modulus. The modulus is proportional to concentration and ex-
pected to scale with a power law exponent of 3/4. The elastic modulus
is expected to exhibit the same behavior but due to the cut-off in the
Kramers-Kronig integral, the reliably measured elastic modulus extends
to about 10 kHz, a frequency apparently still in the transition regime
between collective dynamics and high-frequency single filament dyna-
mics because a true scaling regime would require both moduli to scale
with the same power law. The high-frequency behavior is attributed to
tension in the filaments due to the shear-induced extension. At lower
frequencies, the tension contributes less, and the dominating contribu-
tion to the stress is that of bending and orientational dynamics [1,2].
The data demonstrate that for this system 1-bead MR and 2-bead MR
are in good agreement. This is remarkable since the length scales of
the system, contour length and persistence length, are comparable with
the probe bead diameter. If there was a steric depletion effect, it has
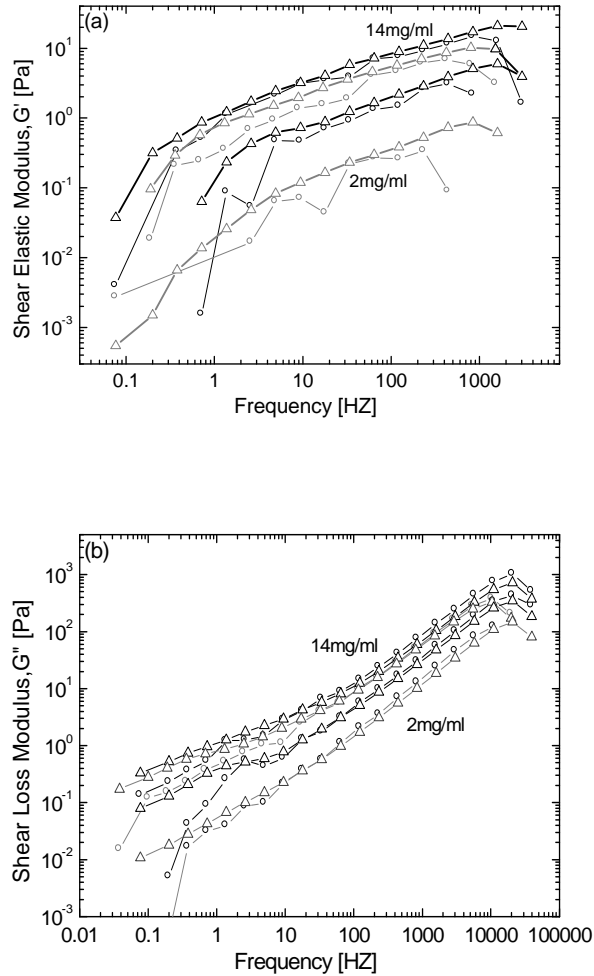evidently led to a negligible effect on the 1-bead results.

Figure 3. (a) The concentration dependence of 1-bead and 2-bead elastic modulus data of $1.16\,\mu$m diameter beads in 2, 5, 10 and $14\,$mg/ml fd solutions. (b) The same for the loss modulus. Pairs of 1-bead (circles) and 2-bead (triangles) moduli are higher for higher concentrations.

Entangled Actin Solutions

Actin is a protein of $42\,$kD molecular weight and a major component of the cytoskeleton of most eukaryotic cells. It forms double-helical filaments of about $7\,$nm diameter, with a persistence length $L_p = 17\,\mu$m, and with a polydisperse length distribution with an average length of approximately $L = 17\,\mu$m in our *in vitro* reconstituted model systems.

Actin stress relaxation is essential for cytoskeleton dynamics and is *in vivo* strictly regulated by a large number of associated regulatory proteins. We study here simplified model systems of just pure actin without additional proteins to explore the fundamental properties and dynamic characteristics of the networks it forms. In contrast to the two systems presented above, characteristic length scales in actin networks are large compared to bead size and we expect interesting differences between 1-bead and 2-bead results, which would report on local network structure near the probes.

Figures 4(a-b) show the results of 1-bead and 2-bead MR for entangled actin networks at $1\,\text{mg/ml}$ actin concentration as a function of bead size. Figure 4(a) shows the elastic shear modulus for 1-bead MR, recorded with various probe bead sizes in comparison with the 2-bead results. Both the 1- and 2-bead curves show the 3/4 power-law scaling at high frequencies, which is expected for semiflexible polymer networks [1,2,4,5]. This regime connects to more complex dynamics with no clear power law characteristics at lower frequencies. There are also clear differences among the results on identical samples, with 1-bead MR systematically underreporting the bulk moduli of the sample in the high frequency regime. These differences between 1-bead and 2-bead MR as well as the systematic trend with probe bead size in the 1-bead results are consistent with the formation of an entropic depletion layer around the beads. The extent of the depletion layer is, roughly speaking, dominated by the shortest of the three characteristic lengths: bead radius, entanglement length and persistence length [1,2,5]. As long as bead size is the shortest length, this depletion layer will dominate the bead response and thereby the 1-bead results. This appears to be the case in the actin networks, and the trend towards less of an influence of local environment with increasing bead size reflects the fact that the other length scales, particularly entanglement length which is estimated to be on the order of 5-10 μm, begin to compete with bead radius. The depletion effect nevertheless does not entirely disappear even at the largest probe size, $D = 5\,\mu$m. This behavior is visible in both the elastic and the loss modulus (Figs. 4(a-b)). A different type of discrepancy is observed at low frequencies within the 1-bead results for the elastic modulus with varying bead size, as well as between 1-bead results with smaller beads and 2-bead results. 2-bead results were independent of bead size and bead distance (after conversion to shear moduli) and the curve shown is the result of averaging data taken at the different bead distances (data for $D = 1.16\,\mu$m bead diameter is shown). We hypothesize that this phenomenon is due to local non-affine deformations of the actin filaments forming the network and will publish further research on these dyna-
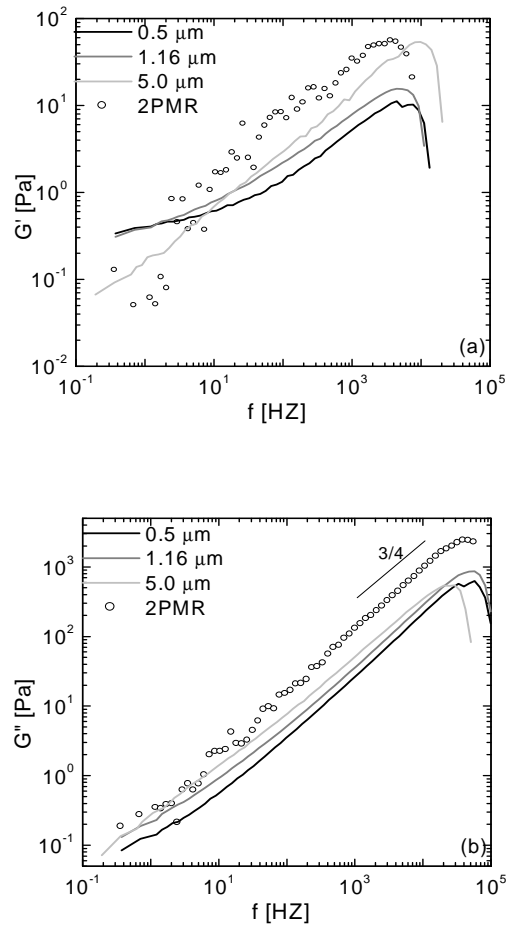
Figure 4. (a) Elastic modulus and (b) loss modulus for 1 mg/ml entangled actin solutions. Comparison of the moduli from 1-bead MR for bead diameters $D = 0.5\mu$ m, $D = 1.16\mu$ m and $D = 5\mu$ m. 2-bead MR data taken at different distances all collapse after scaling by bead distance. Data for bead diameter $D = 1.16\mu$ m is shown.

mics elsewhere. It is important to note that video-based microrheology methods that have also been applied to actin networks will mainly test this regime and may therefore be difficult to interpret.

5.   Conclusions

We have applied a passive microrheology technique, evaluating both single-probe particle fluctuations and correlated two-particle fluctuations to measure the complex shear moduli of solutions of various semiflexible

polymers. Results with fd solutions and worm-like micelle solutions show good agreement between 1-bead and 2-bead MR. This strongly confirms that one can measure bulk viscoelastic properties of these polymer systems with 1-bead MR, which is the simpler and less noisy technique compared to 2-bead MR. Such a confirmation has been lacking up to now. More complex behavior was observed for actin solutions, providing strong evidence for local depletion effects near the bead surface as well as indications of non-affine filament dynamics visible at low frequencies. The results together advocate 1-bead MR as a reliable high resolution and high bandwidth technique to study simple systems far surpassing conventional rheology both in sensitivity and bandwidth. A combination of 1-bead and 2-bead MR, on the other hand, provides a way to explore more complex scale-dependent and local dynamic properties in various polymers, biological and colloidal systems.

Acknowledgments

References

[1] D.C. Morse, *Macromolecules*, Vol.31, pp.7030, 1998.

[2] D.C. Morse, *Macromolecules*, Vol.31, pp.7044, 1998.

[3] A.C. Maggs, *Phys. Rev. E*, Vol.55, pp.7396, 1996.

[4] F. Gittes, F.C. MacKintosh, *Phys. Rev. E*, Vol.58, pp.1241, 1998.

[5] B. Schnurr, F. Gittes, F.C. MacKintosh, et al., *Macromolecules*, Vol.30, pp.7781, 1997.

[6] K. Addas, J.X. Tang, C.F. Schmidt, *Phys. Rev. E*, Vol.70, 021503, 2004.

[7] A. J. Levine and F. Mackintosh, pp.manuscript in preparation.

[8] F. Gittes, C.F. Schmidt, *Method. Cell. Biol.*, Vol.55, pp.129, 1998.

[9] A. J. Levine, T.C. Lubensky, *Phys. Rev. E*, Vol.63(4), 041510, 2001.

[10] M. W. Allersma, F. Gittes, M. J. deCastro, et al., *Biophys. J.*, Vol.74, pp.1074, 1998.

[11] J. F. Berret, J. Appell, G. Porte, Langmuir, Vol.9, pp.2851, 1993.

[12] M. Buchanan, M. Atakhorrami, J.F. Palierne, F.C. Mackintosh, C. F. Schmidt, (manuscript in preparation).